# Adaptive Finite-Time Prescribed Performance Control of Vehicular Platoons With Multilevel Threshold and Asymptotic Convergence

Zhenyu Gao, *Member, IEEE*, Wei Liu, Zhongyang Wei, and Ge Guo, *Senior Member, IEEE*

***Abstract*— This paper studies a prescribed performance platoon control of connected vehicles with multiple performance threshold. A continuous gain function is introduced, combining with finite-time performance function, a novel prescribed performance control (PPC) scheme is developed, which makes the tracking error tend to the prescribed region with different threshold within the user-defined time. Then, a new finite-time reaching law is proposed, based on which, an improved finite-time sliding mode platoon control algorithm is proposed. The suggested control strategy not only ensures the two stability indexes of the platoon system, i.e., finite-time individual vehicle stability and finite-time string stability, but also realizes the asymptotic convergence of the spacing tracking error. Eventually, numerical simulations are carried out, based on which, the feasibility of the proposed scheme are validated.**

***Index Terms*— Vehicular platoon, finite-time stability, sliding mode control, asymptotic convergence, prescribed performance control, multilevel threshold.**

## I. Introduction

OVER the past few years, with the rapid development of economy and the sharp increase of travel demand, the number of private cars has been greatly increased, and with it come serious traffic problems, such as environmental pollution, vehicle congestion and so on [1], [2], [3], [4]. After a long search, it was found that the vehicle driving in a platoon with a small inter-vehicle spacing can effectively alleviate the above problems [5], [6], [7], [8], [9], and hence, the investigation on the platoon control of connected vehicles has sprung up. Vehicular platoon, as a control system, a suitable controller for each vehicle is essential, for which many advanced algorithms have been applied to the platoon system, for example sliding mode control [10], backstepping control [11], model predictive control [12], optimal control [13], [14], [15], and many others. Limited by the feedback structure, only satisfactory steady-state system performance can be obtained by the above methods, while the transient performance is also crucial for the platooning of vehicles [16], [17].

For the sake of addressing this problem, the prescribed performance control (PPC) were adopted, based on which the transient and steady-state performance of the system all be ensured better [17], [18], [19], [20], [21], [22]. To be specific, the work [18] designed a PPC method based on conventional performance function, which can guarantee that the spacing errors evolve with prescribed performance. A finite time performance function is introduced to drive the platoon tracking error converge to a designated region within fixed time in [20] and [22], meanwhile, the work in [22] also eliminate the strict constraints on the initial conditions of the system. However, these works only effective for the platooning of vehicular system with fixed threshold. It is well known that to avoid collisions between adjacent vehicles, the allowable spacing error threshold must be different at high or low speeds, thus, the PPC methods with fixed threshold may leads to an overly conservative choice for parameters, which confines the error to a wide range and impacts the control effect.

The convergence time is another core index to evaluate the vehicle platoon control strategy [23], [24], [25]. Up to today, many advance control methods have been developed, including finite-time controller [21], [22], fixed-time controller [19], [20], and improved versions of the above controllers [24], [25]. Although the desired platoon objective can be achieved within a predefined time by these results, only the boundedness of the tracking errors was ensured. In other words, the errors can only tend to a residual set and cannot approach origin. With the increasing requirements for control accuracy, nothing is more attractive than zero tracking error, which also means that the previous method is no longer applicable. Therefore, it has been found that finite-time asymptotic tracking control of vehicular platoon is a meaningful and unresolved issue, which is another motivation of this article.

In order to response to the shortcomings of the existing results, we will investigate finite-time prescribed performance control of vehicular platoons with dynamic threshold by a novel finite-time asymptotic sliding mode control approach. In comparison with the existing results, the primary contributions are summarized as follows:

Received 28 May 2024; revised 19 October 2024; accepted 24 January 2025. Date of publication 7 February 2025; date of current version 5 May 2025. This work was supported in part by the National Natural Science Foundation of China under Grant 62303101 and in part by the Natural Science Foundation of Hebei Province under Grant F2023501001. The Associate Editor for this article was B. F. Ciuffo. *(Corresponding author: Zhenyu Gao.)*

Zhenyu Gao, Wei Liu, and Zhongyang Wei are with the School of Control Engineering, Northeastern University at Qinhuangdao, Qinhuangdao 066004, China (e-mail: 18840839109@163.com; liu_w1999@163.com; 15953603659@163.com).

Ge Guo is with the State Key Laboratory of Synthetical Automation for Process Industries, Northeastern University, Shenyang 110819, China (e-mail: geguo@yeah.net).

Digital Object Identifier 10.1109/TITS.2025.3536002

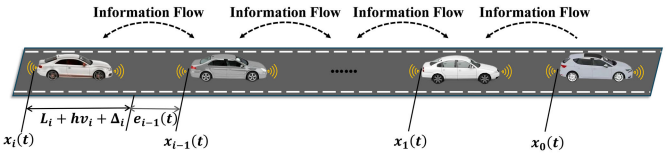


Fig. 1. The heterogeneous vehicular platoon based on bidirectional communication topology.

1) A novel PPC scheme is proposed that synthesizes a continuous gain function together with a newly finite-time performance function, which can guarantee that tracking errors converge to a predefined region with different threshold within user-designed time rather than the prescribed region with fixed threshold [17], [18], [19], [20], [21], [22].
2) A finite-time asymptotic tracking platoon control method in the context of sliding mode control technique is designed for the first time. The proposed control scheme can compel the tracking error converge to a small region nearby zero within settling time, and eventually approach to origin asymptotically, which is a distinct advantage compared with existing finite-time results [21], [22], where only the uniformly ultimately bounded results can be guaranteed.

The rest of this article is assigned as follows. Problem formulation is introduced in Section II. The construct of performance function and error transformation are described in Section III, along with which, the controller design and stability analysis are given in Section IV. In Section V, numerical simulations are carried out to illustrate the effectiveness of the proposed control method. Finally, Section VI summarizes this work.

## II. Problem Formation

As shown in Fig. 1, based on bidirectional (BD) communication topology, a vehicular platoon that is made up by one leader and $N$ following vehicles is considered in this paper.

### A. Vehicle Model

As in [26], the following third-order nonlinear model is adopted for vehicle $i$ $(1 \leq i \leq N)$:

$$\begin{aligned} \dot{x}_i(t) &= v_i(t) \\ \dot{v}_i(t) &= a_i(t) \\ \dot{a}_i(t) &= f_i(v_i, a_i, t) + u_i(t) + \omega_i(t) \end{aligned} \tag{1}$$

where $x_i(t)$, $v_i(t)$, $a_i(t)$ are the position, velocity and acceleration, respectively, $u_i(t)$ is the barking/throttling input, $\omega_i(t)$ is the external disturbance, and $f_i(v_i, a_i, t)$ denotes the unknown nonlinear dynamics, which is expressed as:

$$\begin{aligned} f_i(v_i, a_i, t) = -\frac{1}{m_i \tau_i}\Big[\rho_{ai} A_i C_{ai}\left(\frac{1}{2}v_i^2 + \tau_i v_i a_i\right) \\ + m_i g b_i \cos\delta_i + m_i g \sin\delta_i\Big] - \frac{1}{\tau_i}a_i \end{aligned}$$

wherein the detailed definition of each parameter can be found in Table I.

TABLE I
The Definition of Each Parameter for a Vehicle

| Parameter | Description | Unit |
|---|---|---|
| $m_i$ | Vehicle's mass | $kg$ |
| $\tau_i$ | Engine time constant | $s$ |
| $\rho_{ai}$ | Air density | $kg/m^3$ |
| $\delta_i$ | Road slope angle | $rad$ |
| $C_{ai}$ | Drag coefficient | - |
| $A_i$ | Frontal cross-area | $m^2$ |
| $g$ | Acceleration of gravity | $m/s^2$ |
| $b_i$ | Road resistance coefficient | - |

Inspired by [27], rewrite $f_i(v_i, a_i, t)$ as

$$f_i(v_i, a_i, t) = f_{i0}(v_i, a_i, t) + \Delta f_i(v_i, a_i, t) \tag{2}$$

where $f_{i0}(v_i, a_i, t)$ and $\Delta f_i(v_i, a_i, t)$ represent the known term and the uncertain term, respectively.

Further, the dynamics of vehicle $i$, based on (2), becomes

$$\dot{a}_i(t) = f_{i0}(v_i, a_i, t) + u_i(t) + D_i(t) \tag{3}$$

where $D_i(t) = \Delta f_i(v_i, a_i, t) + \omega_i(t)$ denotes the lumped disturbance acting on vehicle $i$.

*Assumption 1:* The lumped disturbance $D_i$ is bounded and satisfies $|D_i(t)| \leq \bar{D}_i$, where $\bar{D}_i$ is an unknown positive constant.

To generate the reference trajectory for the platoon, the dynamics of leader is described by:

$$\begin{aligned} \dot{x}_0(t) &= v_0(t) \\ \dot{v}_0(t) &= a_0(t). \end{aligned} \tag{4}$$

Based on [26] and [28], by introducing the term $\delta_i(t)$ to remove the assumption that zero initial spacing errors, the following constant time headway policy (CTHP) is defined as:

$$\begin{cases} e_i(t) = \tilde{e}_i(t) - \delta_i(t) \\ \tilde{e}_i(t) = x_{i-1}(t) - x_i(t) - L_i - \Delta_i - h_i v_i(t) \\ \delta_i(t) = \Big\{\tilde{e}_i(0) + \big[\pi_i \tilde{e}_i(0) + \dot{\tilde{e}}_i(0)\big]t + \\ \qquad \frac{1}{2}\big[\pi_i^2 \tilde{e}_i(0) + 2\pi_i \dot{\tilde{e}}_i(0) + \ddot{\tilde{e}}_i(0)\big]t^2\Big\} e^{-\pi_i t} \end{cases} \tag{5}$$

where $L_i$ is the vehicle's length, $h_i$ denotes the time headway, $\Delta_i$ represents the minimum safe distance among adjacent vehicles, and $\pi_i$ is a positive constant. It is easily found that $e_i(0) = 0$, $\dot{e}_i(0) = 0$ and $\ddot{e}_i(0) = 0$.

### B. Control Objectives

In this paper, we focus on develop a new control method in the context of sliding mode control technique for the vehicular platoon described as (1) and (4) such that the following three objectives can be achieved simultaneous.

1) *Finite-time Compound individual vehicle stability:* The inter-vehicle spacing error $e_i$ converges to a small region $\epsilon_i$ within finite time $T_i$, and eventually approaches to zero, that is

$$\begin{cases} \lim\limits_{t \to T_i} |e_i(t)| \leq \epsilon_i \\ \lim\limits_{t \to \infty} |e_i(t)| = 0 \end{cases} \tag{6}$$

where $\epsilon_i$ and $T_i$ are positive constants.

2) *Finite-time String Stability:* After a given time $T_{i\Pi}$, the spacing error $e_i$ satisfies

$$|G_i(s)| = \left|\frac{E_{i+1}(s)}{E_i(s)}\right| \leq 1, \forall\, t \geq T_{i\Pi} \tag{7}$$

where $E_i(s)$ is the Laplace form of $e_i(t)$.

3) *Finite-time prescribed performance:* The tracking error tends to the given region $\left(-\underline{\xi}_i \rho_i(\tilde{T}_i), \bar{\xi}_i \rho_i(\tilde{T}_i)\right)$ within finite-time $\tilde{T}_i > 0$, that is

$$-\underline{\xi}_i \rho_i(t) < e_i(t) < \bar{\xi}_i \rho_i(t), \forall t \geq \tilde{T}_i \tag{8}$$

where $\underline{\xi}_i, \bar{\xi}_i$ are positive constants, and $\rho_i(t)$ is performance function.

In what follows, some useful lemmas and definitions are given for controller design and stability analysis.

*Lemma 1 [29]:* On the set $[0, +\infty)$, If there exist a continuous function $f(t)$ and a constant $\bar{f}$, and satisfies $\lim_{x\to+\infty} \int_0^x f(\tau)d\tau < \bar{f} < \infty$ with $\bar{f}$ a constant. Then, the result $\lim_{t\to+\infty} f(t) = 0$ holds.

*Lemma 2 [30]:* Considering the nonlinear system $\dot{x} = O(x)$. If there exists continuous function $V(x(t)) : R^n \to R^+ \cup \{0\}$, scalars $a_0 < 0$, $\frac{1}{2} < p < 1$ and $b_0 > 0$ such that $\dot{V}(x(t)) \leq e^{-\lambda t}(a_0 V^p(x(t)) + b_0)$. Then, $V(x(t))^p \leq \frac{b_0}{(1-\theta)a_0}$ in finite time, and the convergence time can be defined as

$$T = \frac{1}{\lambda} \ln \frac{\theta a_0}{\frac{\lambda}{1-p}\left(\left(\frac{b_0}{(1-\theta)a_0}\right)^{\frac{1-p}{p}} - V^{1-p}(0)\right) + \theta a_0} \tag{9}$$

where $0 < \theta < 1$.

*Lemma 3 [31]:* Consider the nonlinear system $\dot{x} = O(x)$, and the positive-definite function $V(x)$. If $\dot{V}(x) \leq -\lambda_1 V(x) - \lambda_2 V(x)^\gamma + \eta$ with $\lambda_1 > 0, \lambda_2 > 0, 0 < \gamma < 1$ and $0 < \eta < \infty$, then $\dot{x} = \phi(x)$ is practical finite-time stable (PFnTS), and the residual set of the solution of $\dot{x} = O(x)$ is given by

$$\lim_{t\to T_r} |V(x)| \leq \min\left\{\frac{\eta}{(1-\theta)\lambda_1}, \left(\frac{\eta}{(1-\theta)\lambda_2}\right)^{\frac{1}{\gamma}}\right\} \tag{10}$$

with $\theta$ satisfies $0 < \theta < 1$. The convergence time is bounded by

$$T_r \leq \max\left\{\frac{1}{\theta\lambda_1(1-\gamma)} \ln \frac{\theta\lambda_1 V^{1-\gamma}(0) + \lambda_2}{\lambda_2}, \frac{1}{\lambda_1(1-\gamma)} \ln \frac{\lambda_1 V^{1-\gamma}(0) + \theta\lambda_2}{\theta\lambda_2}\right\}. \tag{11}$$

*Lemma 4 [31]:* Consider the nonlinear system $\dot{x} = O(x)$, and the positive-definite function $V(x)$. If $\dot{V}(x) \leq -\lambda_1 V(x) - \lambda_2 V(x)^\gamma$ with $\lambda_1 > 0$, $\lambda_2 > 0$ and $0 < \gamma < 1$, then $\dot{x} = O(x)$ is global finite-time stable (FnTS), and the settling time can be estimated by

$$T_r \leq \frac{1}{\lambda_1(1-\alpha)} \ln \frac{\lambda_1 V^{1-\alpha}(0) + \lambda_2}{\lambda_2}. \tag{12}$$

*Lemma 5 [21]:* Let $\xi_1, \xi_2, \ldots, \xi_N \geq 0$, then

$$\sum_{i=1}^N \xi_i^p \geq \left(\sum_{i=1}^N \xi_i\right)^p, 0 < p \leq 1. \tag{13}$$

*Lemma 6 [21]:* For $s \leq c, c > 0, q > 0, k > 0, p \geq 0$, we have:

$$s^{1+k} - c^{1+k} \leq (c-s)^{1+k}$$
$$p^k(q-p) \leq \frac{1}{1+k}\left(q^{1+k} - p^{1+k}\right). \tag{14}$$

*Lemma 7 [32]:* For $\forall\sigma > 0$, one has:

$$0 \leq |x| - \frac{x}{\sqrt{x^2+\sigma^2}} \leq \sigma. \tag{15}$$

*Definition 1 [33]:* The continuous function $\rho(t)$ can be called finite-time performance function (FnTPF), if the following conditions are met:

1) $\rho(t) > 0$.
2) $\dot{\rho}(t) \leq 0$.
3) $\rho(t) = \bar{\rho} > 0, \forall t \geq T$, where $\bar{\rho}$ represents any small constant, and $T \geq 0$ represents a given convergence time.

## III. Finite-Time Prescribed Performance Control With Multilevel Threshold

### A. Finite-Time Performance Function Design

To guarantee the spacing error $e_i(t)$ converges to a performance region with different boundary, inspired by [34], the following FnTPF is designed:

$$\rho_i(t) = \rho_{i1}(t) \prod_{j=1}^M \phi_{i,j}(t) \tag{16}$$

with

$$\rho_{i1}(t) = \begin{cases} \dfrac{\lambda_i - \frac{t}{\bar{T}_{i,1}}}{\ln\left(e + \frac{\bar{T}_{i,1}t}{\bar{T}_{i,1}-t}\right)} + \bar{\rho}_{i1}, & 0 \leq t < \bar{T}_{i,1} \\ \bar{\rho}_{i1}, & t \geq \bar{T}_{i,1} \end{cases} \tag{17}$$

and

$$\begin{cases} \underset{j=1}{\phi_{i,j}(t) = 1} \\ \underset{j\geq 2}{\phi_{i,j}(t) =} \begin{cases} 1 - \dfrac{d_{i,j}}{2}\left(1 - \cos\left(\dfrac{\pi}{a_{i,j}}\left(t - \underline{T}_{i,j-1}\right)\right)\right), \\ \qquad t \in [\underline{T}_{i,j-1}, \bar{T}_{i,j}) \\ 1 - d_{i,j}, \\ \qquad t \in [\bar{T}_{i,j}, \underline{T}_{i,j}) \end{cases} \end{cases} \tag{18}$$

where $\lambda_i \geq 1$, $\bar{\rho}_{i1}$, $\tilde{T}_i$, $M$, $a_{i,j}$, $\bar{T}_{i,j}$ and $\underline{T}_{i,j}$ are positive constants. Here, $\bar{\rho}_{i1}$ denotes the threshold at the initial time, $M$ denotes the numbers of threshold, $\prod_1^j (1-d_{i,j})\,\bar{\rho}_{i1}$ is the threshold $j$, $\bar{T}_{i,j}$ and $\underline{T}_{i,j}$ denote the start time and the end time of the threshold $j$ for vehicle $i$, $d_{i,j}$ indicates the adjustment ratio of the threshold from threshold $j-1$ to threshold $j$. If $d_{i,j} > 0$, it represents a decrease in the threshold; otherwise,

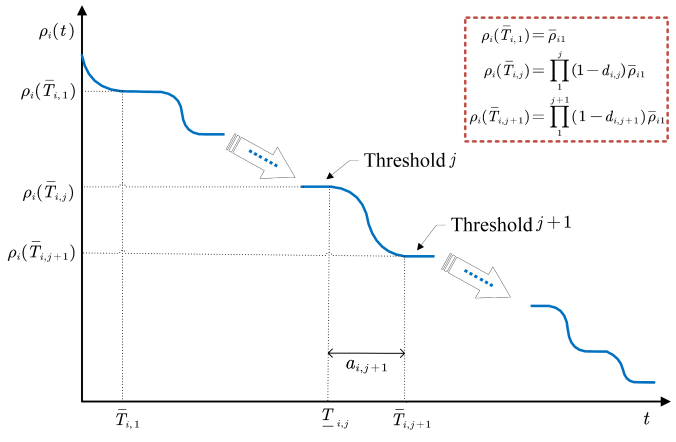


Fig. 2. The diagram of the proposed FnTPF.

it represents an increase. $a_{i,j}$ represents duration of threshold change from threshold $j-1$ to threshold $j$, and satisfies $\bar{T}_{i,j} = \underline{T}_{i,j-1} + a_{i,j}$. The detailed diagram can be seen in Fig. 2.

*Remark 1:* Compared with the FnTPF with fixed threshold in [17], [18], [19], [20], [21], and [22], the gain function $\phi_{i,j}$ is introduced to the FnTPF (16). By adjusting the parameter $d_{i,j}$, the desired threshold can be obtained easily. Meanwhile, the duration of the time-varying process can be regulated only by the parameter $a_{i,j}$.

*Remark 2:* According to (16), it is obvious that $\rho_i(0) = \lambda_i + \bar{\rho}_{i1}$, such that the inequality $-\underline{\xi}_i\rho_i(0) < e_i(0) < \bar{\xi}_i\rho_i(0)$ always holds under the given CTHP (5), removing the restriction of the PF on initial conditions in [18], [19], [20], and [21].

### B. Error Transformation

To fulfill the control goal, the following error transformation is introduced to convert the constrained error into an unconstrained one:

$$\mathcal{E}_i(t) = \Gamma_i^{-1}\left(\frac{e_i(t)}{\rho_i(t)}\right) \tag{19}$$

with

$$\Gamma_i(\mathcal{E}_i) = \frac{\underline{\xi}_i\bar{\xi}_i\left(e^{\mathcal{E}_i} - e^{-\mathcal{E}_i}\right)}{\underline{\xi}_i e^{\mathcal{E}_i} + \bar{\xi}_i e^{-\mathcal{E}_i}} \tag{20}$$

where $\mathcal{E}_i(t)$ denotes the transformed error, and $\Gamma_i^{-1}(\bullet)$ denotes the inverse function of $\Gamma_i(\bullet)$.

Then, one has:

$$\mathcal{E}_i(t) = \frac{1}{2}\ln\frac{\bar{\xi}_i\left(\underline{\xi}_i\rho_i(t) + e_i(t)\right)}{\underline{\xi}_i\left(\bar{\xi}_i\rho_i(t) - e_i(t)\right)}, \tag{21}$$

whose first and second derivatives are derived as follows:

$$\dot{\mathcal{E}}_i(t) = R_i\left(\dot{e}_i(t) - \frac{e_i(t)\dot{\rho}_i(t)}{\rho_i(t)}\right) \tag{22}$$

$$\begin{aligned}\ddot{\mathcal{E}}_i(t) = {} & R_i\left(\ddot{e}_i(t) - \frac{(\dot{e}_i(t)\dot{\rho}_i(t) + e_i(t)\ddot{\rho}_i(t))\rho_i(t)}{\rho_i^2(t)}\right. \\ & \left. + \frac{e_i(t)\dot{\rho}_i^2(t)}{\rho_i^2(t)}\right) + \dot{R}_i\left(\dot{e}_i(t) - \frac{e_i(t)\dot{\rho}_i(t)}{\rho_i(t)}\right)\end{aligned} \tag{23}$$

where $R_i = \frac{\partial\Gamma_i^{-1}}{\partial\left(\frac{e_i(t)}{\rho_i(t)}\right)}\frac{1}{\rho_i(t)} = \frac{1}{2}\left(\frac{1}{e_i(t)+\underline{\xi}_i\rho_i(t)} + \frac{1}{\bar{\xi}_i\rho_i(t)-e_i(t)}\right)$ and $R_i > 0$.

## IV. Controller Design and Stability Analysis

Here, a novel finite-time sliding mode control scheme is developed for the vehicular platoon system that described by (1)-(4). Note that the continuous-time argument $(t)$ is dropped in some cases for the simplicity of notations.

### A. Controller Design

*1) Improved Sliding Mode Surface Design:* To guarantee the convergence of error $\mathcal{E}_i$ with a faster convergence rate, the following sliding mode surface is adopted:

$$S_i = \dot{\mathcal{E}}_i + \alpha_{i1}\psi_i(\mathcal{E}_i) + \alpha_{i2}\mathcal{E}_i \tag{24}$$

with

$$\psi_i(\mathcal{E}_i) = \begin{cases} \text{sig}^{\kappa_i}(\mathcal{E}_i), & |\mathcal{E}_i| \geq \iota_i \\ \beta_{i1}\mathcal{E}_i + \beta_{i2}\mathcal{E}_i^2\text{sign}(\mathcal{E}_i), & |\mathcal{E}_i| < \iota_i \end{cases} \tag{25}$$

where $\alpha_{i1} > 0$, $\alpha_{i2} > \frac{1}{2}$, $\iota_i > 0$, $0 < \kappa_i < 1$, $\beta_{i1} = (2-\kappa_i)\iota_i^{\kappa_i-1}$, $\beta_{i2} = (\kappa_i-1)\iota_i^{\kappa_i-2}$, $\text{sig}^{\kappa_i}(\mathcal{E}_i) = |\mathcal{E}_i|^{\kappa_i}\text{sign}(\mathcal{E}_i)$

In addition, to ensure the string stability of the vehicular platoon, the coupled sliding mode surface technique is introduced:

$$\Pi_i = \begin{cases} q_i S_i - S_{i+1}, & i = 1, 2, \cdots, N-1 \\ q_i S_i, & i = N \end{cases} \tag{26}$$

where $q_i$ is a positive parameter. Note that the convergence of $\Pi_i$ and $S_i$ are same, that is the variables $\Pi_i$ and $S_i$ converge to origin simultaneously.

For the convenience of subsequent controller design, $\dot{\Pi}_i$ is calculated as follows:

$$\dot{\Pi}_i = \begin{cases} q_i\left(\ddot{\mathcal{E}}_i + \alpha_{i1}\dot{\psi}_i(\mathcal{E}_i) + \alpha_{i2}\dot{\mathcal{E}}_i\right) - \dot{S}_{i+1}(t), \\ \quad i = 1, 2, \cdots, N-1; \\ q_i\left(\ddot{\mathcal{E}}_i + \alpha_{i1}\dot{\psi}_i(\mathcal{E}_i) + \alpha_{i2}\dot{\mathcal{E}}_i\right), i = N. \end{cases} \tag{27}$$

*2) Finite-Time Sliding Mode Controller Design:* To achieve the control objective, the following reaching law is introduced:

$$\dot{\Pi}_i = -\sigma_i\left(K_{i1}|\Pi_i|^{p_i}\text{sign}(\Pi_i)\right) \tag{28}$$

where $\sigma_i = e^{-\varpi_i t}$, $K_{i1}$ and $\varpi_i$ are positive constants with $0 < p_i < 1$.

Further, on the basis of (28), the controller $u_i$ and the adaptation law $\dot{\hat{D}}_i$ are designed as follows:

$$\begin{aligned} u_i = {} & \frac{\sigma_i}{q_i h_i R_i}\left[K_{i1}|\Pi_i|^{p_i}\text{sign}(\Pi_i) + Z_i\right] \\ & + \frac{q_i h_i R_i\hat{\dot{D}}_i}{\sqrt{\Pi_i^2 + \sigma_i^2}} + \frac{K_{i1}|\Pi_i|^{p_i}\text{sign}(\Pi_i)}{q_i h_i R_i} \end{aligned} \tag{29}$$

$$\hat{\dot{D}}_i = \frac{q_i h_i R_i \Pi_i}{\sqrt{\Pi_i^2 + \sigma_i^2}} - \sigma_i K_{i2}\hat{\dot{D}}_i^{p_i} \tag{30}$$

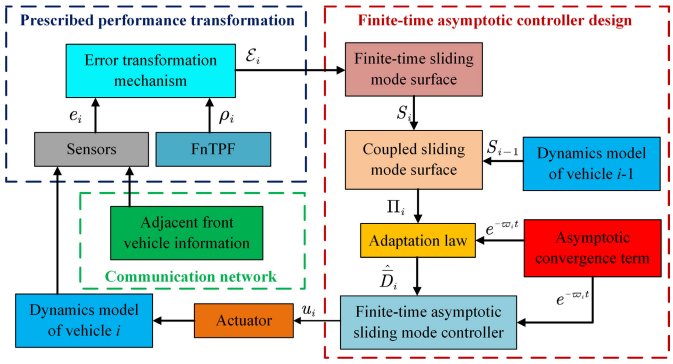


Fig. 3. Control structure diagram of the developed algorithm.

where $K_{i2}$ is a positive constant, and $Z_i$ is given by

$$Z_i = \begin{cases} q_i \left[ R_i \left( -\dfrac{(\dot{e}_i \dot{\rho}_i + e_i \ddot{\rho}_i)\rho_i - e_i \dot{\rho}_i^2}{\rho_i^2} \right) \right. \\ \quad + R_i \left( a_{i-1} - a_i - \ddot{\delta}_i \right) - h_i R_i f_{i0}(v_i, a_i) \\ \quad \left. + \left( \dot{R}_i + \alpha_{i2} R_i \right) \left( \dot{e}_i - \dfrac{e_i \dot{\rho}_i}{\rho_i} \right) + \alpha_{i1} \dot{\psi}_i \right] \\ \quad - \dot{S}_{i+1}, \quad i = 1, 2, \cdots, N-1, \\ q_i \left[ R_i \left( -\dfrac{(\dot{e}_i \dot{\rho}_i + e_i \ddot{\rho}_i)\rho_i - e_i \dot{\rho}_i^2}{\rho_i^2} \right) \right. \\ \quad + R_i \left( a_{i-1} - a_i - \ddot{\delta}_i \right) - h_i R_i f_{i0}(v_i, a_i) \\ \quad \left. + \left( \dot{R}_i + \alpha_{i2} R_i \right) \left( \dot{e}_i - \dfrac{e_i \dot{\rho}_i}{\rho_i} \right) + \alpha_{i1} \dot{\psi}_i \right], i = N. \end{cases} \tag{31}$$

The flowchart of the developed finite-time asymptotic tracking platoon control scheme is displayed in Fig. 3.

### B. Stability Analysis

*Theorem 1:* Consider the vehicular platoon control system (1)-(4) based on CTHP strategy (5) and satisfying Assumption 1. Under the action of the given control scheme, including the performance functions (16)-(18), error transformation (19)-(21), improved sliding mode surface (24), (25), coupled sliding mode surface (26), finite-time asymptotic convergence controller (29) and adaptive law (30), the following three statements hold.

1) All signals of the closed-loop vehicular system can converge to the neighborhood of the origin within a time $T_i$. Meanwhile, the tracking errors $e_i$ $(1 \le i \le N)$ will tend to zero in the end.
2) Finite-time string stability can be guaranteed if the parameter $q_i$ satisfies $0 < q_i < 1$.
3) The performance constraint with multilevel threshold also can be ensured with finite-time.

*Proof:* The proof of *Theorem 1* is accomplished through the following three parts.

***Part 1: Compound individual vehicle stability:*** As in [24] and [29], the following Lyapunov function is considered:

$$V_{i\Pi} = \frac{1}{2}\Pi_i^2 + \frac{1}{2}\tilde{\bar{D}}_i^2 \tag{32}$$

where $\tilde{\bar{D}}_i = \bar{D}_i - \hat{\bar{D}}_i$ is the estimation error.

Taking the time derivative of $V_i$ yields:

$$\dot{V}_{i\Pi} = \Pi_i \dot{\Pi}_i - \tilde{\bar{D}} \dot{\hat{\bar{D}}}. \tag{33}$$

Combining (1), (3), (27) and (29), the time derivative of $\dot{\Pi}_i(t)$ is given as follow:

$$\begin{aligned} \dot{\Pi}_i(t) &= -q_i h_i R_i (u_i + D_i) + Z_i \\ &= -\left[ (1+\sigma_i) K_{i1} |\Pi_i|^{p_i} \operatorname{sign}(\Pi_i) + Z_i + \frac{q_i h_i R_i \hat{\bar{D}}_i}{\sqrt{\Pi_i^2 + \sigma_i^2}} \right] \\ &\quad - q_i h_i R_i D_i + Z_i \\ &= -\left[ (1+\sigma_i) K_{i1} |\Pi_i|^{p_i} \operatorname{sign}(\Pi_i) + \frac{q_i h_i R_i \hat{\bar{D}}_i}{\sqrt{\Pi_i^2 + \sigma_i^2}} \right] \\ &\quad - q_i h_i R_i D_i. \end{aligned} \tag{34}$$

Then, we have

$$\begin{aligned} \Pi_i \dot{\Pi} &= -(1+\sigma_i) K_{i1} |\Pi_i|^{p_i} \Pi_i \operatorname{sign}(\Pi_i) \\ &\quad - \frac{q_i h_i R_i \hat{\bar{D}}_i \Pi_i}{\sqrt{\Pi_i^2 + \sigma_i^2}} - q_i h_i R_i D_i \Pi_i. \end{aligned} \tag{35}$$

Based on (30), (33) and (35), one has

$$\begin{aligned} \dot{V}_{i\Pi} &= -(1+\sigma_i) K_{i1} |\Pi_i|^{p_i} \Pi_i \operatorname{sign}(\Pi_i) \\ &\quad - \frac{q_i h_i R_i \hat{\bar{D}}_i \Pi_i}{\sqrt{\Pi_i^2 + \sigma_i^2}} - q_i h_i R_i D_i \Pi_i \\ &\quad - \frac{q_i h_i R_i \tilde{\bar{D}}_i \Pi_i}{\sqrt{\Pi_i^2 + \sigma_i^2}} + \sigma_i K_{i2} \tilde{\bar{D}}_i \hat{\bar{D}}_i^{p_i} \\ &= -(1+\sigma_i) K_{i1} |\Pi_i|^{p_i} \Pi_i \operatorname{sign}(\Pi_i) \\ &\quad + \sigma_i K_{i2} \tilde{\bar{D}}_i \hat{\bar{D}}_i^{p_i} - \frac{q_i h_i R_i \bar{D}_i \Pi_i}{\sqrt{\Pi_i^2 + \sigma_i^2}} - q_i h_i R_i D_i \Pi_i. \end{aligned} \tag{36}$$

According to Assumption 1, the following inequality can be obtained:

$$-q_i h_i R_i \Pi_i D_i \le q_i h_i R_i \bar{D}_i |\Pi_i|. \tag{37}$$

Using Lemma 7, one has:

$$q_i h_i R_i \bar{D}_i |\Pi_i| - \frac{q_i h_i R_i \bar{D}_i \Pi_i}{\sqrt{\Pi_i^2 + \sigma_i^2}} \le q_i h_i R_i \bar{D}_i \sigma_i. \tag{38}$$

On the grounds of Lemma 6, $\tilde{\bar{D}}_i \hat{\bar{D}}_i^{\rho}$ satisfies the following inequality:

$$\hat{\bar{D}}_i^{p_i} \left( \bar{D}_i - \hat{\bar{D}}_i \right) \le -\frac{1}{1+p_i} \tilde{\bar{D}}_i^{1+p_i} + \frac{2}{1+p_i} \bar{D}_i^{1+p_i}. \tag{39}$$

Substituting (37), (38) and (39) into (36), one has:

$$\begin{aligned} \dot{V}_{i\Pi} &\le -(1+\sigma_i) K_{i1} |\Pi_i|^{p_i+1} - \frac{\sigma_i K_{i2}}{1+p_i} \tilde{\bar{D}}_i^{1+p_i} \\ &\quad - \frac{\sigma_i K_{i2}}{1+p_i} 2 \bar{D}_i^{1+p_i} + q_i h_i R_i \bar{D}_i \sigma_i. \end{aligned} \tag{40}$$

Further, we can have

$$\dot{V}_{i\Pi} \le -\sigma_i \left[ K_{i1} 2^{\frac{1+p_i}{2}} \left( \frac{\Pi_i^2}{2} \right)^{\frac{1+p_i}{2}} + \frac{K_{i2}}{1+p_i} 2^{\frac{1+p_i}{2}} \left( \frac{\tilde{\bar{D}}_i^2}{2} \right)^{\frac{1+p_i}{2}} \right] + \sigma_i \left( q_i h_i R_i \bar{D}_i - \frac{K_{i2}}{1+p_i} 2 \bar{D}_i^{1+p_i} \right) - K_{i1} |\Pi_i|^{p_i+1}. \tag{41}$$

Then

$$\dot{V}_{i\Pi} \le -(\sigma_i + 1)\eta_i \left( \frac{\Pi_i^2}{2} \right)^{\frac{1+p_i}{2}} - \sigma_i \eta_i \left( \frac{\tilde{\bar{D}}_i^2}{2} \right)^{\frac{1+p_i}{2}} + \sigma_i \varrho_i \tag{42}$$

where

$$\eta_i = \min \left\{ K_{i1} 2^{\frac{1+p_i}{2}}, \frac{K_{i2}}{1+p_i} 2^{\frac{1+p_i}{2}} \right\}$$
$$\varrho_i = q_i h_i R_i \bar{D}_i - \frac{K_{i2}}{1+p_i} 2 \bar{D}_i^{1+p_i}. \tag{43}$$

In the light of Lemma 5, we have

$$\dot{V}_{i\Pi} \le -\sigma_i \eta_i \left[ \left( \frac{\Pi_i^2}{2} \right) + \left( \frac{\tilde{\bar{D}}_i^2}{2} \right) \right]^{\frac{1+p_i}{2}} + \sigma_i \varrho_i = -\sigma_i \eta_i V_{i\Pi}^{\frac{1+p_i}{2}} + \sigma_i \varrho_i. \tag{44}$$

According to Lemma 2, it is conclude that $V_{i\Pi}$ is finite-time stable, thus, the signals $\Pi_i$ and $\tilde{\bar{D}}_i$ will converge to the compact set $\Omega_i$ within finite time $T_{i\Pi}$, wherein $\Omega_i$ and $T_{i\Pi}$ are expressed as follows:

$$\left\{ |\Pi_i|, |\tilde{\bar{D}}_i| \right\} \le \Omega_i := \sqrt[\frac{1+p_i}{2}]{\frac{\varrho_i}{(1-\theta_i)\eta_i}} \tag{45}$$

and

$$T_{i\Pi} \le \frac{1}{\varpi_i} \ln \frac{\theta_i \eta_i}{\frac{2\varpi_i}{1-p_i} \left( V_{i\Pi}^{\frac{1-p_i}{2}}(0) + \left( \frac{\varrho_i}{(1-\theta_i)\eta_i} \right)^{\frac{1-p_i}{1+p_i}} \right) + \theta_i \eta_i} \tag{46}$$

where $0 < \theta_i < 1$.

Furthermore, from (42), it yields

$$\dot{V}_{i\Pi} \le -\eta_i \left( \frac{\Pi_i^2}{2} \right)^{\frac{1+p_i}{2}} + \sigma_i \varrho_i. \tag{47}$$

Integrate (47) from 0 to $t$:

$$V_{i\Pi}(t) - V_{i\Pi}(0) \le \int_0^t -\eta_i \left( \frac{\Pi_i^2}{2} \right)^{\frac{1+p_i}{2}} + \sigma_i \varrho_i d\tau. \tag{48}$$

Then

$$\eta_i \int_0^t \left( \frac{\Pi_i^2}{2} \right)^{\frac{1+p_i}{2}} d\tau \le V_{i\Pi}(0) + \varrho_i \frac{1 - e^{-\varpi_i t}}{\varpi_i}. \tag{49}$$

Further, we have

$$\lim_{t \to +\infty} \eta_i \int_0^t \left( \frac{\Pi_i^2}{2} \right)^{\frac{1+p_i}{2}} d\tau \le V_{i\Pi}(0) + \frac{\varrho_i}{\varpi_i} < \infty. \tag{50}$$

By using Lemma 1, we can infer that $\lim_{t \to \infty} \Pi_i = 0$. Based on above analysis, one can obtain

$$\begin{cases} \lim_{t \to T_{i\Pi}} |\Pi_i| = \Omega_i \\ \lim_{t \to \infty} |\Pi_i| = 0. \end{cases} \tag{51}$$

Since $\Pi_i$ and $S_i$ have the same convergence, thus there exists a positive constant $\Delta_i$ such that

$$\begin{cases} \lim_{t \to T_{i\Pi}} |S_i| = \Delta_i \\ \lim_{t \to \infty} |S_i| = 0. \end{cases} \tag{52}$$

Next, the convergence of $\mathcal{E}_i$ will be proved by the following two discussions.

**Discussion 1:** When $S_i = \Delta_i$, sliding mode surface (24) can be rewritten as:

$$\dot{\mathcal{E}}_i = -\alpha_{i1} \psi_i(\mathcal{E}_i) - \alpha_{i2} \mathcal{E}_i + \Delta_i. \tag{53}$$

Consider the following Lyapunov function

$$V_{i\mathcal{E}} = \frac{1}{2} \mathcal{E}_i^2 \tag{54}$$

and taking the time derivative of $V_{i\mathcal{E}}$, one has

$$\dot{V}_{i\mathcal{E}} = \mathcal{E}_i \dot{\mathcal{E}}_i. \tag{55}$$

Based on the relationships between $|\mathcal{E}_i|$ and $\iota_i$ in (25), the convergence of $\mathcal{E}_i$ will be discussed by the following two cases.

*Case 1:* if $|\mathcal{E}_i| \ge \iota_i$, one can obtain

$$\dot{\mathcal{E}}_i = -\alpha_{i1} \mathrm{sig}^{\kappa_i}(\mathcal{E}_i) - \alpha_{i2} \mathcal{E}_i + \Delta_i. \tag{56}$$

Substituting (56) into (55) yields

$$\begin{aligned} \dot{V}_{i\mathcal{E}} &= -\alpha_{i1} \mathcal{E}_i \mathrm{sig}^{\kappa_i}(\mathcal{E}_i) - \alpha_{i2} \mathcal{E}_i^2 + \Delta_i \mathcal{E}_i \\ &\le -2^{\frac{\kappa_i+1}{2}} \alpha_{i1} \left( \frac{1}{2} \mathcal{E}_i^2 \right)^{\frac{\kappa_i+1}{2}} - 2\alpha_{i2} \left( \frac{1}{2} \mathcal{E}_i^2 \right) + \Delta_i \mathcal{E}_i \\ &\le -2^{\frac{\kappa_i+1}{2}} \alpha_{i1} V_{i\mathcal{E}}^{\frac{\kappa_i+1}{2}} - 2\alpha_{i2} V_{i\mathcal{E}} + \Delta_i \mathcal{E}_i \\ &\le -2^{\frac{\kappa_i+1}{2}} \alpha_{i1} V_{i\mathcal{E}}^{\frac{\kappa_i+1}{2}} - 2\alpha_{i2} V_{i\mathcal{E}} + \frac{1}{2} \Delta_i^2 + \frac{1}{2} \mathcal{E}_i^2 \\ &\le -\bar{\alpha}_{i1} V_{i\mathcal{E}}^{(\kappa_i+1)/2} - \bar{\alpha}_{i2} V_{i\mathcal{E}} + \frac{1}{2} \Delta_i^2 \end{aligned} \tag{57}$$

with $\bar{\alpha}_{i1} = 2^{\frac{\kappa_i+1}{2}} \alpha_{i1}$ and $\bar{\alpha}_{i2} = (2\alpha_{i2} - 1)$.

Based on Lemma 3, $\mathcal{E}_i$ is practical finite-time convergent when $|\mathcal{E}_i| \ge \iota_i$, and $|\mathcal{E}_i|$ approaches to the following region with given time $T_{i\mathcal{E}}$:

$$\lim_{t \to T_{i\mathcal{E}}} |\mathcal{E}_i| \le \Psi_i = \min \left\{ \sqrt{\frac{\Delta_i^2}{(1-\zeta_i)\bar{\alpha}_{i2}}}, \sqrt{2 \left( \frac{\Delta_i^2}{2(1-\zeta_i)\bar{\alpha}_{i1}} \right)^{\frac{2}{\kappa_i+1}}} \right\} \tag{58}$$

with $0 < \zeta_i < 1$, and the settling time $T_{i\mathcal{E}}$ is bounded by

$$T_{i\mathcal{E}} \le \max \left\{ \frac{2}{\zeta_i \bar{\alpha}_{i2} (1-\kappa_i)} \ln \frac{\zeta_i \bar{\alpha}_{i2} V_{i\mathcal{E}}^{\frac{1-\kappa_i}{2}}(0) + \bar{\alpha}_{i1}}{\bar{\alpha}_{i1}}, \right.$$

$$\left.\frac{2}{\bar{\alpha}_{i2}(1-\kappa_i)}\ln\frac{\bar{\alpha}_{i2}V_{i\mathcal{E}}^{\frac{1-\kappa_i}{2}}(0)+\zeta_i\bar{\alpha}_{i1}}{\zeta_i\bar{\alpha}_{i1}}\right\}. \quad (59)$$

*Case 2:* if $|\mathcal{E}_i| < \iota_i$, one has

$$\dot{\mathcal{E}}_i = -\alpha_{i1}\left(\beta_{i1}\mathcal{E}_i + \beta_{i2}\mathcal{E}_i^2\text{sign}(\mathcal{E}_i)\right) - \alpha_{i2}\mathcal{E}_i + \Delta_i. \quad (60)$$

Since $\dot{\mathcal{E}}_i = -\alpha_{i1}\left(\beta_{i1}\mathcal{E}_i + \beta_{i2}\mathcal{E}_i^2\text{sign}(\mathcal{E}_i)\right) - \alpha_{i2}\mathcal{E}_i + \Delta_i$ has a faster convergence rate than $\dot{\mathcal{E}}_i = -\alpha_{i1}\text{sig}^{\kappa_i}(\mathcal{E}_i) - \alpha_{i2}\mathcal{E}_i + \Delta_i$, there is a smaller convergence time in this stage.

According to above analysis, it is concluded that $\mathcal{E}_i$ converges to the region $\Psi_i$ when $t \geq T_i \geq T_{i\Pi} + T_{i\mathcal{E}}$.

**Discussion 2:** When $S_i = 0$ as shown in (52), sliding mode surface (24) becomes

$$\dot{\mathcal{E}}_i = -\alpha_{i1}\psi_i(\mathcal{E}_i) - \alpha_{i2}\mathcal{E}_i. \quad (61)$$

Here, the analysis of $\mathcal{E}_i$ is same with **Discussion 1**, thus it is omitted here.

By applying Lemma 4, $\mathcal{E}_i$ converges to zero in finite time $T_{i\mathcal{E}}$, satisfies

$$T_{i\mathcal{E}} \leq \frac{1}{\alpha_{i2}(1-\kappa_i)}\ln\frac{2\alpha_{i2}V_{i\mathcal{E}}^{(1-\kappa_i)/2}(0)+2^{(\kappa_i+1)/2}\alpha_{i1}}{2^{(\kappa_i+1)/2}\alpha_{i1}}. \quad (62)$$

On the basis of the above analysis, the following results hold:

$$\begin{cases}\lim\limits_{t\to T_i}|\mathcal{E}_i| \leq \Psi_i \\ \lim\limits_{t\to\infty}|\mathcal{E}_i| = 0.\end{cases} \quad (63)$$

Due to both variables $e_i(t)$ and $\mathcal{E}_i$ are equivalent, thus the compound individual vehicle stability (6) is guaranteed.

***Part 2: Finite-time String stability:*** The proof is along similar lines as in [22], [26], [28], [35], and [36]. Since $\Pi_i = q_i S_i - S_{i+1}$, once $\Pi_i$ converges to the origin, we have

$$q_i S_i = S_{i+1} \quad (64)$$

which illustrates that $\frac{S_{i+1}}{S_i} = q_i$. Since $q_i \in (0, 1]$, then $0 < \frac{S_{i+1}}{S_i} \leq 1$.

The conclusion can be obtained based on [22], thus it is omitted here.

*Remark 3:* Different from the most existing works [19], [20], [21], [22], [24], [25], [30], [31], benefiting from the term $\sigma_i = e^{-\varpi_i t}$, the ideal result $S_i = 0$ can be obtained instead of $S_i \approx 0$, which makes a positive effect on the string stability of the platoon system, and more importantly, it greatly improves the control accuracy and the result of zero steady-state tracking error can be obtained.

***Part 3: Reachability of prescribed performance (8):*** According to ***Part 1: Compound individual vehicle stability***, the tracking error $\mathcal{E}_i(t)$ is finite-time convergent and bounded, thus there must exists a maximum value. Here, defining $\bar{\mathcal{E}}_i$ as the upper bound of $\mathcal{E}_i$.

From (21), it is deduced that:

$$\frac{\bar{\xi}_i\left(\underline{\xi}_i\rho_i(t) + e_i(t)\right)}{\underline{\xi}_i\left(\bar{\xi}_i\rho_i(t) - e_i(t)\right)} = e^{2\mathcal{E}_i}. \quad (65)$$

Then

$$\frac{e_i(t)+\underline{\xi}_i\rho_i(t)}{\bar{\xi}_i\rho_i(t)+\underline{\xi}_i\rho_i(t)} = \frac{\underline{\xi}_i e^{2\mathcal{E}_i}}{\bar{\xi}_i+\underline{\xi}_i e^{2\mathcal{E}_i}}. \quad (66)$$

Due to $\bar{\mathcal{E}}_i \geq \mathcal{E}_i$, we have

$$0 < \frac{\xi_i e^{-2\bar{\mathcal{E}}_i}}{\bar{\xi}_i+\xi_i e^{-2\bar{\mathcal{E}}_i}} < \frac{\xi_i e^{2\mathcal{E}_i}}{\bar{\xi}_i+\underline{\xi}_i e^{2\mathcal{E}_i}} < \frac{\xi_i e^{2\bar{\mathcal{E}}_i}}{\bar{\xi}_i+\xi_i e^{2\bar{\mathcal{E}}_i}} < 1. \quad (67)$$

Further, it follows that $0 < \frac{e_i(t)+\underline{\xi}_i\rho_i(t)}{\bar{\xi}_i\rho_i(t)+\underline{\xi}_i\rho_i(t)} < 1$, so $-\underline{\xi}_i\rho_i(t) < e_i(t) < \bar{\xi}_i\rho_i(t)$.

According to the characteristic of (16), it is obvious that the tracking error $e_i(t)$ converges to the region $\left(-\underline{\xi}_i\rho_i(\tilde{T}_i), \bar{\xi}_i\rho_i(\tilde{T}_i)\right)$ within finite-time $\tilde{T}_i > 0$. Therefore, the predefined tracking performance (8) can be guaranteed.

The whole proof of Theorem 1 is accomplished by the above three parts. ■

## V. Simulation Studies

In this section, we conduct numerical simulations for the vehicular platoon system with $N = 5$ following vehicles and one leader to demonstrate the effectiveness of the developed scheme. Here, the vehicle parameters are selected as: $m_i = 1600kg$, $A_i = 2.2m^2$, $\rho_{ai} = 0.2$, $\tau_i = 0.2$, $C_{ai} = 0.35$, $g = 9.8m/s^2$, $\delta_i = 0$, $b_i = 0.02$, $\omega_i = 0.1\tanh(t)$, $\Delta f_i(v_i, a_i) = 0.5 f_{i0}(v_i, a_i)$, and the platoon parameters are chosen as: $\Delta_i = 7m$, $h_i = 1s$, $L_i = 2m$ and $\pi_i = 1$, The initial states (i.e., positions and velocities) are selected as: $x_i(0) = [45, 36.2, 27.5, 17.8, 9.2, 0]m$, and $v_i(0) = 0m/s$ with $i = 0, 1, \cdots, N$.

The acceleration of leader is designed as:

$$a_0(t) = \begin{cases}0.5t\ m/s^2, & 0s \leq t < 4s \\ 2\ m/s^2, & 4s \leq t < 8s \\ -0.5t + 6\ m/s^2, & 8s \leq t \leq 12s \\ 0\ m/s^2, & t \geq 12s\end{cases} \quad (68)$$

### A. Simulation Results of the Proposed Method

Here, the control parameters of each vehicle are designed as: $q_i = 0.9$, $\kappa_i = 0.8$, $\alpha_{i1} = 12$, $\alpha_{i2} = 8$, $\iota_i = 0.1$, $\underline{\xi}_i = \bar{\xi}_i = 0.4$, $K_{i1} = 3$, $K_{i2} = 80$, $\varpi_i = 0.03$, $p_i = 0.999$.

The dynamic threshold FnTPF parameters are designed as: $\bar{T}_{i,1} = 20$, $\lambda_i = 1$, $a_{i,1} = 6$, $\bar{\rho}_{i1} = 1$, $\underline{T}_{i,1} = 30$, $d_{i,1} = 0.6$.

The simulation results are depicted in Fig. 4. The trajectory of each vehicle is presented in Fig. 4(a), which illustrates that the desired platoon configuration can be achieved in finite time and no collision occurs between inter-vehicles. Figs. 4(b) and 4(c) give the velocity and acceleration information of each vehicle, respectively, from which we can see that these two states of each vehicle tend to coincide in a finite time. Figs. 4(d) and 4(e) show the sliding mode surface $S_i$ and tracking error $e_i$, it is obvious that these two variables converge to small region nearby zero within finite time. From Fig. 4(g), it is concluded that the tracking errors are always within the predefined region, and no boundary violation occurs. Furthermore, of significant importance is the clear influence

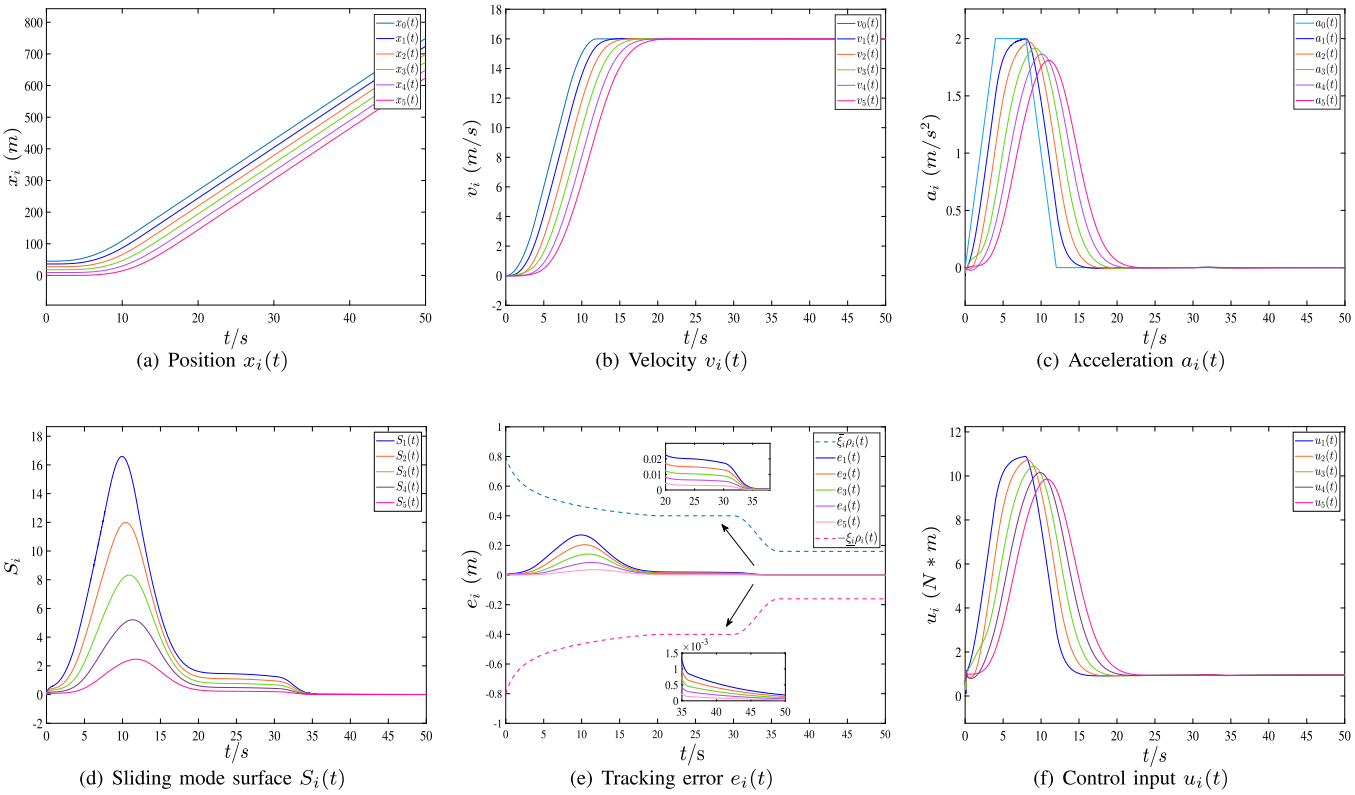


(a) Position $x_i(t)$ (b) Velocity $v_i(t)$ (c) Acceleration $a_i(t)$

(d) Sliding mode surface $S_i(t)$ (e) Tracking error $e_i(t)$ (f) Control input $u_i(t)$

Fig. 4. Simulation results of the proposed method.

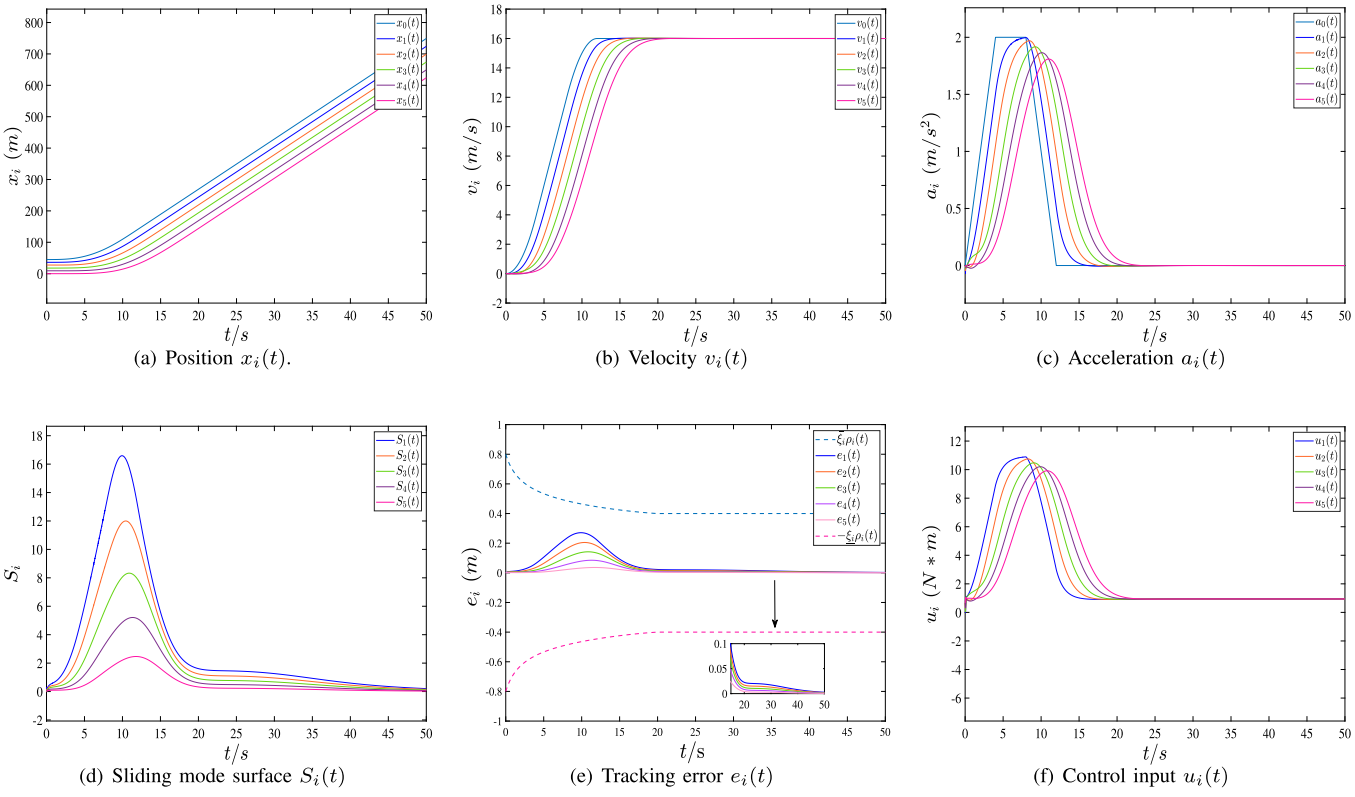


(a) Position $x_i(t)$. (b) Velocity $v_i(t)$ (c) Acceleration $a_i(t)$

(d) Sliding mode surface $S_i(t)$ (e) Tracking error $e_i(t)$ (f) Control input $u_i(t)$

Fig. 5. Simulation results of Case 1.

of the dynamic threshold predefined performance function on the tracking error. Importantly, it can be clearly seen that the tracking error becomes smaller as the threshold is adjusted, which indicates that our given PPC algorithm is efficient.

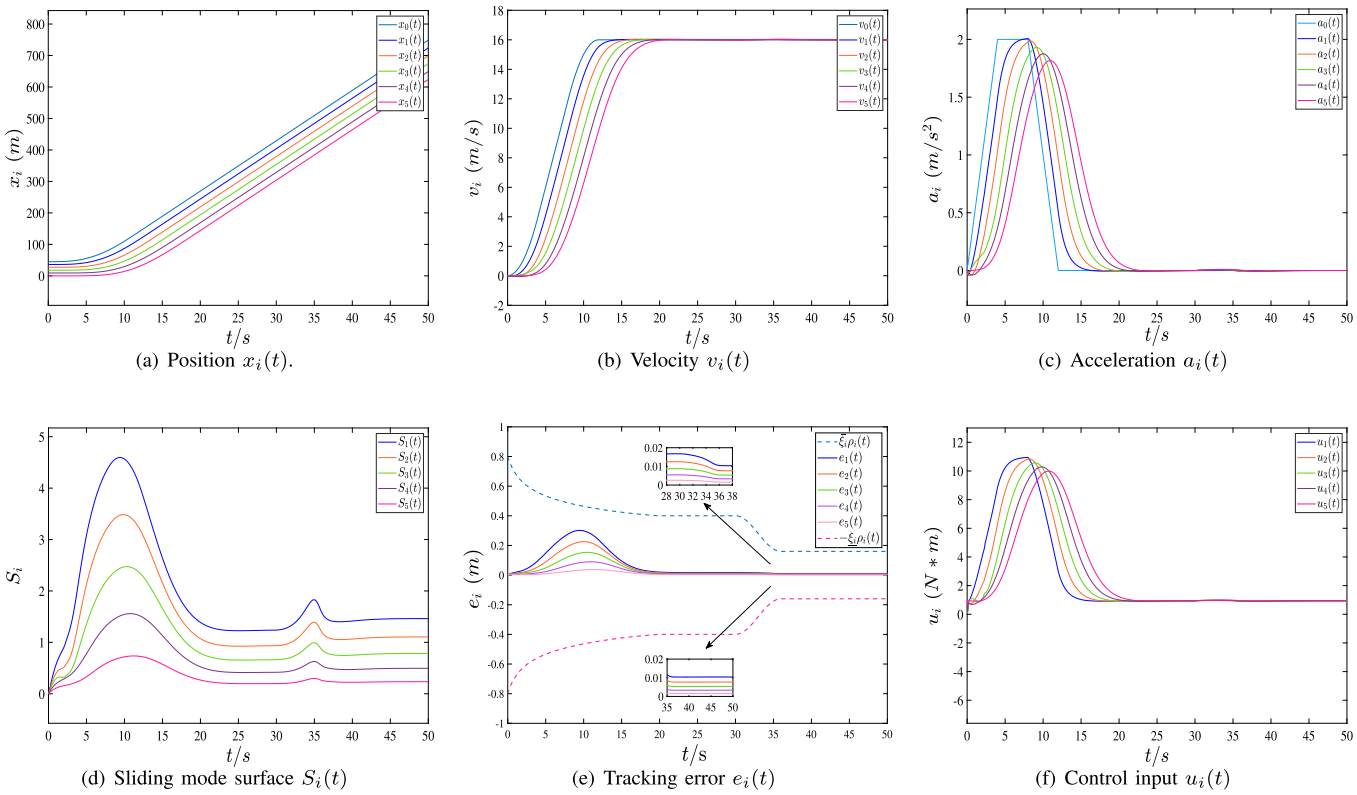


(a) Position $x_i(t)$. (b) Velocity $v_i(t)$ (c) Acceleration $a_i(t)$

(d) Sliding mode surface $S_i(t)$ (e) Tracking error $e_i(t)$ (f) Control input $u_i(t)$

Fig. 6. Simulation results of Case 2.

In addition, the platoon string stability is also guaranteed, i.e., $|e_{i+1}(t)| < |e_i(t)|$ with $i = 1, 2, 3, 4$. The control input is depicted in Fig. 4(f), and we can find that once the platoon reaches stability, the output value of controller remains constant.

### B. Comparison With Different Methods

In this subsection, two contrasting cases are considered to validate the benefits of the algorithm proposed in this paper.

**Case 1:** Comparison with the existing FnTPF with the fixed threshold.

Here, the conventional FnTPF proposed in [22] is considered:

$$\rho_i(t) = \begin{cases} \dfrac{1-\frac{t}{20}}{\ln\left(e+\frac{20t}{20-t}\right)}+1, & 0 \le t < 20s \\ 1, & t \ge 20s \end{cases} \tag{69}$$

and other control parameters are the same as those selected in the Subsection *A. Simulation Results of the Proposed Method*.

Simulation results are shown in Fig. 5, which shows that the desired platoon objectives also can be realized. It can be observed from Figs. 4(e) and 5(e) that the proposed method in this paper has a positive effect on the error convergence, that is, smaller transient error and faster convergence rate can be obtained.

**Case 2:** Comparison with the existing finite time sliding mode control scheme.

In this part, to contrast with the previous finite-time control scheme, the following reaching law given in [37] is considered:

$$\dot{\Pi}_i = -K_{i1}\,|\Pi_i|^{p_i}\,\mathrm{sign}\,(\Pi_i) - L_{i1}\Pi_i. \tag{70}$$

Here, $L_{i1} = 5$, and other parameters are selected the same with Subsection A.

The simulation results are depicted in Fig. 6. By comparing the curves of tracking error $e_i$ given in Figs. 4(e) and 6(e), we can see that although the two control schemes can drive the tracking error $e_i$ converge to a small region in finite time, zero tracking error also can be obtained under the given scheme in this paper. In conclusion, the proposed control algorithm in this work has better performance in control accuracy, convergence rate, performance constraints and so on.

## VI. Conclusion

Toward better control accuracy and faster convergence, the tracking problem of vehicular platoon system subject to multilevel prescribed performance constraints is studied. By combining conventional finite-time performance function and novel continuous gain function, a new finite-time performance function is designed to compel the tracking errors converge to a predefined region with multiple performance threshold within finite time. Then, a new finite time sliding mode control scheme is developed, with which the tracking error tends to a small region near zero in finite time and eventually converge zero. In addition, string stability and reachability of prescribed performance are also guaranteed.

It is noteworthy that there is a limitation in this paper that the convergence time depends on the initial conditions of the system, thus our future research will focus on eliminating this constraint.

## REFERENCES


[1] S. Chu and A. Majumdar, "Opportunities and challenges for a sustainable energy future," *Nature*, vol. 488, no. 7411, pp. 294–303, Aug. 2012.

[2] J. Rios-Torres and A. A. Malikopoulos, "A survey on the coordination of connected and automated vehicles at intersections and merging at highway on-ramps," *IEEE Trans. Intell. Transp. Syst.*, vol. 18, no. 5, pp. 1066–1077, May 2017.

[3] A. Rasouli and J. K. Tsotsos, "Autonomous vehicles that interact with pedestrians: A survey of theory and practice," *IEEE Trans. Intell. Transp. Syst.*, vol. 21, no. 3, pp. 900–918, Mar. 2020.

[4] Y. Liu, C. Zong, C. Dai, H. Zheng, and D. Zhang, "Behavioral decision-making approach for vehicle platoon control: Two noncooperative game models," *IEEE Trans. Transport, Electrific.*, vol. 9, no. 3, pp. 4626–4638, Sep. 2023.

[5] B. Paden, M. Čáp, S. Z. Yong, D. Yershov, and E. Frazzoli, "A survey of motion planning and control techniques for self-driving urban vehicles," *IEEE Trans. Intell. Vehicles*, vol. 1, no. 1, pp. 33–55, Mar. 2016.

[6] Y. Zheng, S. E. Li, K. Li, F. Borrelli, and J. K. Hedrick, "Distributed model predictive control for heterogeneous vehicle platoons under unidirectional topologies," *IEEE Trans. Control Syst. Technol.*, vol. 25, no. 3, pp. 899–910, May 2017.

[7] S. Wen and G. Guo, "Control of leader-following vehicle platoons with varied communication range," *IEEE Trans. Intell. Vehicles*, vol. 5, no. 2, pp. 240–250, Jun. 2020.

[8] Y. Yan, H. Du, Q.-L. Han, and W. Li, "Discrete multi-objective switching topology sliding mode control of connected autonomous vehicles with packet loss," *IEEE Trans. Intell. Veh.*, vol. 8, no. 4, pp. 2926–2938, Apr. 2023.

[9] B.-F. Yue and W.-W. Che, "Data-driven dynamic event-triggered fault-tolerant platooning control," *IEEE Trans. Ind. Informat.*, vol. 19, no. 7, pp. 8418–8426, Jul. 2023.

[10] Z. Liu and H. Pan, "Barrier function-based adaptive sliding mode control for application to vehicle suspensions," *IEEE Trans. Transport. Electrific.*, vol. 7, no. 3, pp. 2023–2033, Sep. 2021.

[11] L. Zhang et al., "An adaptive backstepping sliding mode controller to improve vehicle maneuverability and stability via torque vectoring control," *IEEE Trans. Veh. Technol.*, vol. 69, no. 3, pp. 2598–2612, Mar. 2020.

[12] M. Wang, C. Zhao, J. Xia, and J. Sun, "Periodic event-triggered robust distributed model predictive control for multiagent systems with input and communication delays," *IEEE Trans. Ind. Informat.*, vol. 19, no. 11, pp. 11216–11228, Nov. 2023.

[13] T. Liu, L. Cui, B. Pang, and Z.-P. Jiang, "A unified framework for data-driven optimal control of connected vehicles in mixed traffic," *IEEE Trans. Intell. Vehicles*, vol. 8, no. 8, pp. 4131–4145, Aug. 2023.

[14] S. E. Li, R. Li, J. Wang, X. Hu, B. Cheng, and K. Li, "Stabilizing periodic control of automated vehicle platoon with minimized fuel consumption," *IEEE Trans. Transport. Electrific.*, vol. 3, no. 1, pp. 259–271, Mar. 2017.

[15] H. Zhang, J. Peng, H. Dong, F. Ding, and H. Tan, "Integrated velocity optimization and energy management strategy for hybrid electric vehicle platoon: A multiagent reinforcement learning approach," *IEEE Trans. Transport. Electrific.*, vol. 10, no. 2, pp. 2547–2561, Jun. 2024.

[16] Q. Zeng and J. Zhao, "Event-triggered adaptive finite-time control for active suspension systems with prescribed performance," *IEEE Trans. Ind. Informat.*, vol. 18, no. 11, pp. 7761–7769, Nov. 2022.

[17] C.-L. Zhang and G. Guo, "Prescribed performance sliding mode control of vehicular platoons with input delays," *IEEE Trans. Intell. Transp. Syst.*, vol. 25, no. 9, pp. 11068–11076, Sep. 2024.

[18] D. Li and G. Guo, "Prescribed performance concurrent control of connected vehicles with nonlinear third-order dynamics," *IEEE Trans. Veh. Technol.*, vol. 69, no. 12, pp. 14793–14802, Dec. 2020.

[19] Z. Gao, Y. Zhang, and G. Guo, "Adaptive fixed-time sliding mode control of vehicular platoons with asymmetric actuator saturation," *IEEE Trans. Veh. Technol.*, vol. 72, no. 7, pp. 8409–8423, Jul. 2023.

[20] Z. Gao, Y. Zhang, and G. Guo, "Fixed-time prescribed performance adaptive fixed-time sliding mode control for vehicular platoons with actuator saturation," *IEEE Trans. Intell. Transp. Syst.*, vol. 23, no. 12, pp. 24176–24189, Dec. 2022.

[21] Z. Gao, Y. Zhang, and G. Guo, "Finite-time fault-tolerant prescribed performance control of connected vehicles with actuator saturation," *IEEE Trans. Veh. Technol.*, vol. 72, no. 2, pp. 1438–1448, Feb. 2023.

[22] Z. Sun, Z. Gao, G. Guo, and S. Wen, "Finite-time control of vehicular platoons with global prescribed performance and actuator nonlinearities," *IEEE Trans. Intell. Vehicles*, vol. 9, no. 1, pp. 1768–1779, Jan. 2024.

[23] J. Han, J. Zhang, C. He, C. Lv, X. Hou, and Y. Ji, "Distributed finite-time safety consensus control of vehicle platoon with senor and actuator failures," *IEEE Trans. Veh. Technol.*, vol. 72, no. 1, pp. 162–175, Jan. 2023.

[24] Z. Gao, Y. Zhang, and G. Guo, "Prescribed-time control of vehicular platoons based on a disturbance observer," *IEEE Trans. Circuits Syst. II, Exp. Briefs*, vol. 69, no. 9, pp. 3789–3793, Sep. 2022.

[25] J. Wang, X. Luo, W.-C. Wong, and X. Guan, "Specified-time vehicular platoon control with flexible safe distance constraint," *IEEE Trans. Veh. Technol.*, vol. 68, no. 11, pp. 10489–10503, Nov. 2019.

[26] G. Guo, P. Li, and L.-Y. Hao, "A new quadratic spacing policy and adaptive fault-tolerant platooning with actuator saturation," *IEEE Trans. Intell. Transp. Syst.*, vol. 23, no. 2, pp. 1200–1212, Feb. 2022.

[27] V. K. Tripathi, A. K. Kamath, L. Behera, N. K. Verma, and S. Nahavandi, "An adaptive fast terminal sliding-mode controller with power rate proportional reaching law for quadrotor position and altitude tracking," *IEEE Trans. Syst., Man, Cybern., Syst.*, vol. 52, no. 6, pp. 3612–3625, Jun. 2022.

[28] G. Guo, P. Li, and L.-Y. Hao, "Adaptive fault-tolerant control of platoons with guaranteed traffic flow stability," *IEEE Trans. Veh. Technol.*, vol. 69, no. 7, pp. 6916–6927, Jul. 2020.

[29] Z. Gao, X. Li, Z. Wei, and G. Guo, "Adaptive fuzzy finite-time asymptotic tracking control of vehicular platoons with nonsmooth asymmetric input nonlinearities," *IEEE Trans. Intell. Transp. Syst.*, vol. 25, no. 11, pp. 19062–19072, Nov. 2024.

[30] Y. Li, Y.-X. Li, and S. Tong, "Event-based finite-time control for nonlinear multiagent systems with asymptotic tracking," *IEEE Trans. Autom. Control*, vol. 68, no. 6, pp. 3790–3797, Jun. 2023.

[31] A. Polyakov, "Nonlinear feedback design for fixed-time stabilization of linear control systems," *IEEE Trans. Autom. Control*, vol. 57, no. 8, pp. 2106–2110, Aug. 2012.

[32] Z. Ma and H. Ma, "Adaptive fuzzy backstepping dynamic surface control of strict-feedback fractional-order uncertain nonlinear systems," *IEEE Trans. Fuzzy Syst.*, vol. 28, no. 1, pp. 122–133, Jan. 2020.

[33] Y. Liu, X. Liu, and Y. Jing, "Adaptive neural networks finite-time tracking control for non-strict feedback systems via prescribed performance," *Inf. Sci.*, vol. 468, pp. 29–46, Nov. 2018.

[34] X. Liu, H. Zhang, J. Sun, and X. Guo, "Dynamic threshold finite-time prescribed performance control for nonlinear systems with dead-zone output," *IEEE Trans. Cybern.*, vol. 54, no. 1, pp. 655–664, Jan. 2024.

[35] J. Wang, X. Luo, J. Yan, and X. Guan, "Distributed integrated sliding mode control for vehicle platoons based on disturbance observer and multi power reaching law," *IEEE Trans. Intell. Transp. Syst.*, vol. 23, no. 4, pp. 3366–3376, Apr. 2022.

[36] C. Pan, Y. Chen, Y. Liu, and I. Ali, "Adaptive resilient control for interconnected vehicular platoon with fault and saturation," *IEEE Trans. Intell. Transp. Syst.*, vol. 23, no. 8, pp. 10210–10222, Aug. 2022.

[37] Y. Li, Y. Zhao, W. Liu, and J. Hu, "Adaptive fuzzy predefined-time control for third-order heterogeneous vehicular platoon systems with dead zone," *IEEE Trans. Ind. Informat.*, vol. 19, no. 9, pp. 9525–9534, Sep. 2023.

**Zhenyu Gao** (Member, IEEE) received the Ph.D. degree from Dalian Maritime University, Dalian, China, in 2019.

He is currently an Associate Professor with the School of Control Engineering, Northeastern University at Qinhuangdao. His current research interests include cooperative control of autonomous vehicles and intelligent transportation systems.

**Wei Liu** received the B.S. degree from Dalian Polytechnic University in 2022. He is currently pursuing the M.S. degree with the School of Control Engineering, Northeastern University at Qinhuangdao.

His research interests include vehicular platoon control and intelligent transportation systems.

**Zhongyang Wei** received the B.S. degree from Shandong University of Science and Technology in 2022. He is currently pursuing the M.S. degree with the School of Control Engineering, Northeastern University at Qinhuangdao.

His research interests include vehicular platoon control and intelligent transportation systems.

**Ge Guo** (Senior Member, IEEE) received the B.S. and Ph.D. degrees from Northeastern University, China, in 1994 and 1998, respectively.

He is currently a Professor with Northeastern University. He has published over 200 international journal articles within his areas of interest, which include intelligent transportation systems and cyber-physical systems.

Dr. Guo won a series of awards, including the CAA Young Scientist Award, the First Prize of Natural Science Award of Hebei Province, and the First Prize of Science and Technology Progress Award of Gansu Province. He is an Associate Editor of IEEE TRANSACTIONS ON INTELLIGENT TRANSPORTATION SYSTEMS, IEEE TRANSACTIONS ON VEHICULAR TECHNOLOGY, IEEE TRANSACTIONS ON INTELLIGENT VEHICLES, the *Information Sciences*, *IEEE Intelligent Transportation Systems Magazine*, the *Acta Automatica Sinica*, *China Journal of Highway and Transport*, and the *Journal of Control and Decision*.